Journal of Applied Sciences and Nanotechnology, Vol. 1, No. 2 (2021)

Journal of Applied Sciences and Nanotechnology

Journal homepage: https://jasn.uotechnology.edu.iq/

Investigation of Morphological, Optical, and Antibacterial Properties of Hybrid ZnO-MWCNT Prepared by Sol-gel

Zahraa S. Sh. Khedaer, Duha S. Ahmed, Selma M. H. Al-Jawad*

Applied Physics Division/ Department of Applied Sciences, University of Technology, Baghdad – Iraq

Article information

Article history:
Received: April, 13, 2021
Accepted: April, 29, 2021
Available online: June, 25, 2021

Keywords:
Multiwalled carbon nanotubes,
ZnO-MWCNT hybrid,
Sol-Gel,
Structural and optical properties,
Antibacterial activity

Corresponding Author:
Selma M. H. Al-Jawad
salma_aljawad@yahoo.com

Abstract

In this research, raw multiwalled carbon nanotubes (R-MWCNT) was successfully functionalized using sulfuric acid and nitric acid. Then a hybrid (ZnO-MWCNT) synthesized by the sol-gel method where diethylene glycol was used as a solvent and stabilizer that works to prevent the accumulation of nanoparticles and reduces the viscosity of the solution. A group of diagnostic techniques, including XRD, UV-Vis, EDX and microscopy has recognized the structural and optical properties of the prepared nanoparticles. High Resolution Electronic Scanner (FE-SEM) was also used in the investigation. FE-SEM images showed the formation of the hybrid (ZnO-MWCNT) by the growth of spherical clusters on the surface of the cross-linked tubes (MWCNT). In addition, FE-SEM images confirmed the success of a ZnO-MWCNT hybrid. The emergence of spherical shapes deposited on cylindrical tubes and associated with a wrinkled surface was recognized. In addition, the particle size ratio increased. The UV-Vis spectra revealed that all the composites had good absorbency with a shift towards short wavelengths. While it was observed from the analysis of X-ray diffraction (XRD) the formation of a hexagonal wurtzite crystal structure due to zinc oxide with a polycrystalline nature. The average crystal size calculated from the Debye-spark equation increased with the increase in the concentration of the streaked material. Antibacterial activity was studied for all prepared samples against *Escherichia coli* (*E. coli*) and *Staphylococcus aureus* (*S. aureus*) at different µg/ml concentrations (500, 750, and 1000). It was observed that the highest inhibition Zone for functionalized multiwalled carbon nanotubes (F-MWCNT) and ZnO-MWCNT hybrid was (17.3, 12.3mm), (22.5, 19mm) for *Escherichia coli* and *Staphylococcus aureus*, respectively.

DOI: 10.53293/jasn.2021.11634, Department of Applied Science, University of Technology

1. Introduction

Nanotechnology has been significantly developed in the last decade and has become widely used in many fields of life such as environmental protection, health care, energy, agriculture, transportation, consumer products, medical devices, computers [1]. The materials used in nanotechnology underwent various chemical or physical processes to produce materials that have good properties such as small size, high surface area, and more effectiveness [2]. Most of the nanomaterials are made of carbon. Carbon appears in various forms, in the form of cylindrical tubes called carbon nanotubes (CNTs), in the form of hollow spheres called fluorine, in the form of flat multi-layer sheets called graphene [3]. Carbon nanotubes (CNTs) are more effective and applicable compared to other nanomaterials. Carbon nanotubes (CNTs) consist of a group of cylindrical layers warped with a nanoscale diameter up to 0.4nm. Multi walled carbon nanotubes (MWCNTs) are a promising material in many areas of life because of their remarkable properties such as high tensile strength, high optical transmission, gas absorption, and high electrical conductivity [4]. MWCNTs are a semiconductor or metallic material depending on the chirality. Carbon nanotubes are used in the synthesis of nanoparticles, which is due to the lower dispersion, less aggregation, and the presence of van der Waals forces [5]. The performance of multiwalled Carbon nanotubes (MWCNTs) was improved by interacting with other nanoparticles to produce a nanocomposite with excellent electrical, thermal and mechanical properties, in addition to a high surface area [6]. Finally, the synthesis of nanocomposite using Multi walled Carbon nanotubes is gaining amazing interest in electronic, medical, commercial, and environmental applications. MWCNTs also have a hydrophobic feature, which makes less reactive and thus low rate of commercial use [7]. Therefore, researchers tended to functionalize carbon nanotubes with organic materials to add functional groups to the surface of MWCNTs to become more active. Another boost is combining MWCNTs with semiconductors produces new nanocomposite that plays an important role in many applications. Most of the semiconductors decorated onto the surface of the MWCNTs are (ZnO, TiO_2, SnO_2, CdS, CdTe) [8-11]. Among the semiconductors mentioned, zinc oxide (ZnO) was used in this study because of its amazing properties such as high stability, high mechanical strength, high piezoelectric properties, and good optical quality [12]. ZnO as a metal oxide II–VI semiconductor has a wide direct band gap of 3.37 eV and has a high electron hole binding energy (60 meV) [11]. The advantage of the wide band gap of zinc oxide makes it a great interest in the manufacture of optoelectronic devices due to its ability to reduce electronic noise, maintain high voltages, and to work at high energy. The advantage of high exciton binding energy gives it an effective role as an excellent fluorescence agent because the capability of stabilizing electron-hole pair recombination [13]. ZnO has amazing advantages such as bio-safety, lower cost, chemical stability, high sensitivity, ease of synthesis, biocompatibility, paramagnetic nature, and wide radiation absorption range. Because of the unique properties that zinc oxide has, it is therefore considered the best semiconductor compared to other oxides [14]. Zinc oxide nanoparticles absorb ultraviolet radiation typically in the range (40-100) nanometers and disperse them. They are therefore used as sunscreens, and since they are invisible on the skin, this makes them commercially desirable [15]. Also, they are used in piezoelectric sensing and mechanical actuators because they have strong thermal and piezoelectric properties resulting from the large electromechanical coupling and the absence of a center of symmetry in the wurtzite structure [16]. Zinc oxide has attracted the interest of applied studies in recent years because it is used in many industries such as pharmaceuticals, food, ceramics, rubber, plastics, printing inks, cement, and dyes. Moreover, zinc oxide nanoparticles are environmentally friendly, so they can play an effective role in biomedical applications such as antibacterial, deodorant, dandruff treatment, and skin irritation. As well as, the form of creams and ointments to accelerate wound healing due to their effective effect antimicrobial. They are used in energy collecting devices due to the semiconductor and piezoelectric properties. They have also been widely used as food preservative and components in food packaging due to high activity against food-borne bacteria [17]. The incorporation of ZnO nanoparticles in MWCNTs is expected to produce a novel hybrid material by doping zinc oxide nanoparticles with transition elements. With their wide interest in many fields, especially in the field of anatomy medicine, because of their ability introduce ferromagnetic behaviour and improving optical, electrical and structural properties [18]. Several recent studies showed a great interest in using multi walled carbon nanotubes as anti-microbial agent due to their low cost, having excellent physical properties, and their adjustable morphology [19]. ZnO- MWCNTs hybrid shows high photo-inactivation of the bacterial cells. In this study, the treatment and modifying of the R-MWCNTs using the acid treatment, and hybrid material, ZnO/MWCNTs was introduced by using sol-gel method and the anti-bacterial activity were studied. In addition, the properties of R-MWCNTs, F-MWCNTs, and hybrid material including crystalline structure, particle size, and morphology were recognized through various characteristic techniques. In addition, the preparation of ZnO\MWCNT hybrid and its analysis

through XRD, FE-SEM and UV-Vis techniques has been carried out. On the other hand, the biological activity of the R-MWCNTs, F-MWCNTs, and ZnO\MWCNT hybrid were studied by the antibacterial activity using diffusion well method against *E. coli* and *P. aeruginosa* bacteria with using different concentrations.

2. Experimental Part

2.1 Acid Treatment of R-MWCNTs

Multiwalled carbon nanotubes (MWCNTs, purity: 95%wt (USA), outside diameter: 5-15 nm) were covalently functionalized by chemical oxidation method to enhance the solubility of MWCNTs in aqueous media and next step for hybrid preparation. High dispersion results have reported with the method. In this part, Raw-MWCNTs were treated by using a mixture of sulphuric acid and nitric acid (3:1 v/v). Firstly, 2g of raw-MWCNTs was functionalized with 150 ml of sulphuric acid (95% H_2SO_4) and 50 ml of nitric acid (65% HNO_3). The mixture was placed in ultra-sonically vibrated in water ultrasonic bath at temperature of 30 °C for 60 min. Then the mixture was diluted with 500 ml of distilled water, vacuum-filtered through a 0.22 μm polycarbonate membrane and then dried at 100 °C for 12 h. The resultant F-MWCNTs was treated with hydrogen peroxide (30% v/v H_2O_2) as reduction reagent, and the same procedure was repeated in order to achieve whole oxidative procedure started via H_2SO_4 and HNO_3. As a second step, but in a gentler manner carboxyl groups were created on the surface of MWCNTs, which could subsequently be dispersed in composite preparation. Thereafter, the solid was washed by deionized water (DI), and then dried at 100 °C for 12 h to produce functional groups like -OH and/or -COOH functionalized F-MWCNTs. The flow chart representing the steps of functionalized F-MWCNTs by using mixture of sulphuric acid and nitric acid and filtrated method is shown in Figure 1.

2.2 Synthesis of ZnO-MWCNTs Hybrid

In this part, ZnO-MWCNTs hybrid was prepared by sol-gel method. Zinc acetate ($Zn(CH_3COO)_2.2H_2O$), multiwalled carbon nanotube (MWCNTs), diethylene glycol ($C_4H_{10}O_3$), and absolute ethanol were used as reactants. Initially, 0.33g of zinc acetate ($Zn(CH_3COO)_2.2H_2O$) was dissolved in 75 ml diethylene glycol (DEG, $C_4H_{10}O_3$), then 3 ml deionized water was added to the solution. Then, the solution of zinc acetate was constantly stirred at 160-180 °C for 12 min. According to the appropriate proportion, the zinc acetate is completely dissolved in a beaker and stirred constantly to get a homogenous solution, and then kept at room temperature for 2h to get ZnO sol. Specific amount of functional MWCNTs was added into the running synthetic solution of ZnO NPs after the gel formation and sonicated for 20 min. The mass of MWCNTs was 0.12 g to obtain the mass ratio of (MWCNTs:ZnO = 1:1). After that, the solution stirred at 160-180 °C for 2 h and then cooled down to the room temperature. Finally, and yet importantly, black precipitate centrifuged and washed with deionized water and absolute ethanol, then dried in an oven at temperature of 60 °C for 48 h. The mixture then calcined at 450 °C for 2h in atmospheric pressure to obtain powder of ZnO-MWCNTs hybrid.

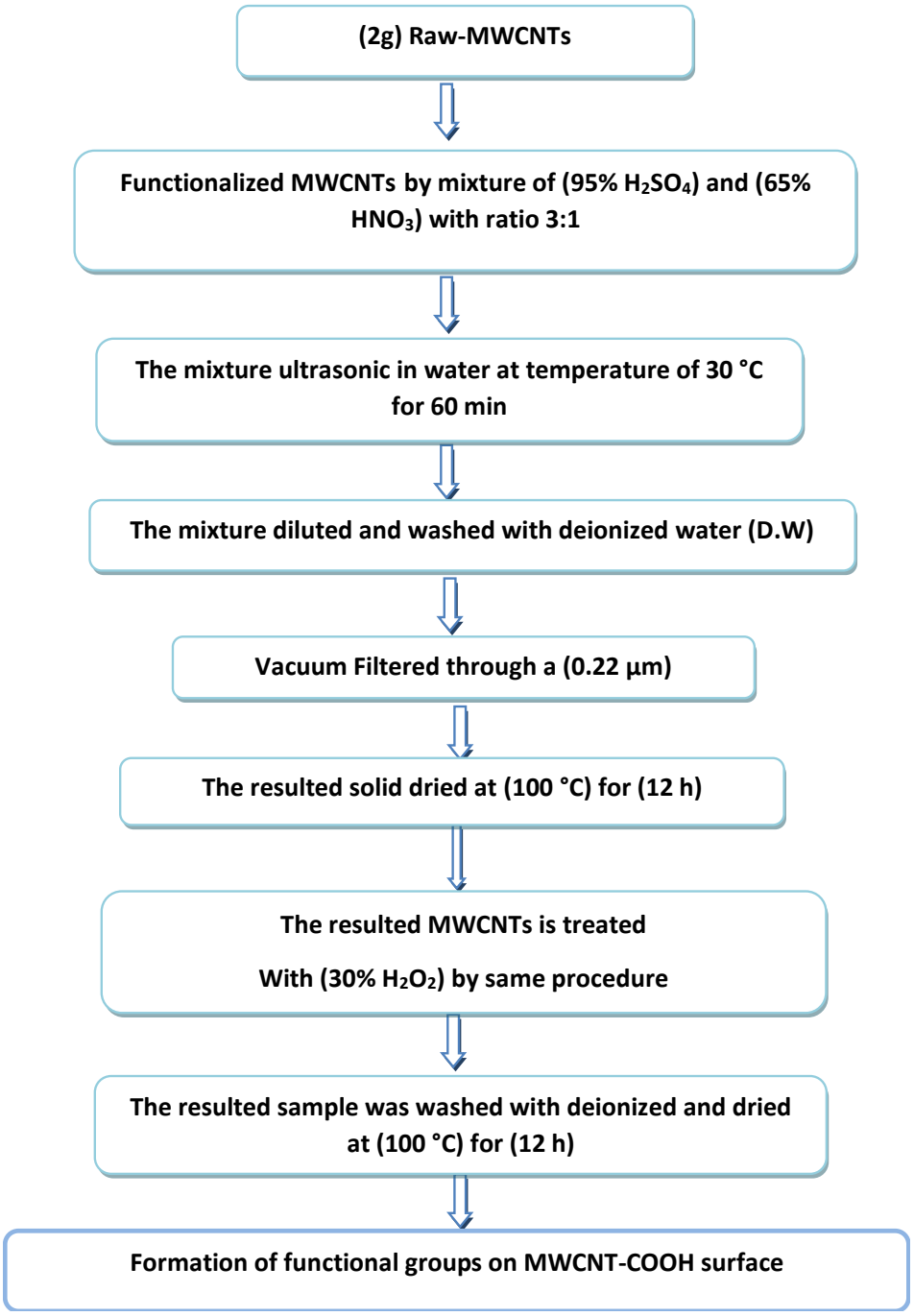

Figure 1: Schematic diagram of represents functionalized method by using concentrated mixture of sulfuric acid and nitric.

2.3 Material Characterization

Zinc acetate (Zn $(CH_3COO)_2.2H_2O$, Sigma-Aldrich, USA), Diethylene glycol (DEG, $C_4H_{10}O_3$, Sasma, Netherlands), multiwalled carbon nanotubes (purity >95 wt%; diameter ~8-15 nm; length ~10-50 µm; Ash<1.5 wt%, Cheaptubes.com Grafton, USA), Sulphuric acid, J.T. Baker, USA. Nitric acid (CDH, India), Hydrogen peroxide (GCC, China) and Cellulose nitrate filter (0.22 µm, Sartorius, German). All solutions used directly without primary purification. The crystal composition of the prepared nanocomposite was determined by X- ray diffraction (XRD) analysis (XRD-6000, Shimadzu, Japan) with Cu Kα radiation (λ=1.54056 Å) at a scanning rate of 0.03° s^{-1} for 2θ in a range from 20° to 80°. The morphology and grain particles of prepared ZnO-MWCNT hybrid noted by field emission scanning electron microscopy (FE-SEM, Mira3- XMU, and Czech)

worked at an acceleration voltage of 30 kV. The UV-Visible spectroscopy accomplished by UV-1800 spectrophotometer (Lambda 750, Perkin Elmer, and Taiwan) in the wavelength range of 200- 800 nm with 10 mm quartz cuvette.

2.4 Inhibition Zone Test (IZ)

The test of Antibacterial effect by measuring the inhibition Zone on agar plates was achieved by using well diffusion method to determine the (IZ) for preparation of different samples and also hybrid materials like ZnO-MWCNTs, F-MWCNTs and R-MWCNTs, respectively, against Gram negative (*E. coli*) bacteria and Gram positive (*S. aureus*) bacteria. Three different concentrations of each sample were used (500, 750, 1000 µg/ml) against the bacteria. The activated bacterial culture (*S. aureus* and *E. coli*) was subcultured on nutrient agar at 37 ^{o}C for overnight, and then bacteria suspended in normal saline (0.9%w\v) to prepare initial concentration of 107-108 CFU/ml of each bacteria strain using (standard McFarland tube 0.5). Each culture spread on nutritious agar plates. Then, different concentrations (500, 750, and 1000 µg/ml) of each sample were poured into well in the whole plates and incubated over night at 37 °C. The inhibition zone diameter of each sample was pendent in millimeter; also, the average of inhibition zones around three wells was determined.

3. Results and Discussion

X-ray diffraction analysis is a technique for identifying the crystal structure and grain size of the synthesized nanomaterials. Figure 2 shows the XRD patterns of diffraction for the R-MWCNTs, F-MWCNTs and ZnO/MWCNTs hybrid, respectively. The XRD patterns of the R-MWCNTs display the appearance of a broad peak of high intensity at 2θ = 25.8° corresponding to the interlayer distance of 3.44 Å. Additionally, the diffraction peak is low intensity at 2θ = 43^{o} and both are related to hkl planes of (002), (100), respectively. After acid treatment of F-MWCNTs, the XRD patterns display a broad diffraction peak at 2θ = 26^{o} corresponding to the interlayer distance of 3.45 Å and a low intensity diffraction peak at 2θ = 43.20^{o} corresponding to the interlayer distance of 2.07 Å, both are related to the hkl planes of (002), (100), respectively, and in good agreement with (JCPDS-0646). A significant shift was observed in the diffraction peak 2θ = 43.20^{o}, owing to the presence of functional oxygen groups that increase the interlayer distance between the F-MWCNTs layers. This reveals the success of the functional process using sulfuric and nitric acid without altering the structure of the F-MWCNTs. It was observed that the average crystal size of the R-MWCNTs and F-MWCNTs are (3.27, 3.19 nm), respectively. In contrast, the XRD analysis of the ZnO/F-MWCNTs hybrid materials was shown in Figure 2. A broad diffraction peak appears at 2θ = 26^{o} corresponding to the interlayer distance of 3.42 Å which is attributed to the hkl planes of (002) of the F-MWCNTs. While the diffraction peaks at 2θ = 31.78^{o}, 34.57^{o}, 36.50^{o}, 48.47^{o}, 59.45^{o}, 63.91^{o}, and 67.54^{o} corresponding to (100), (002), (101), (102), (110), (103) and (112) planes, respectively. This indicates the hexagonal wurtzite structure of ZnO through the identical peaks with the peaks of the standard sample (JCPDS card No. 36-1451). The average crystal size was calculated by the Scherer's equation (1) [19, 20].

$$D = \frac{k\lambda}{\beta \cos\theta} \qquad \text{..... (1)}$$

Where: D represents particle size; k is a dimensionless shape factor, with a value close to unity. The shape factor has a typical value of about 0.9, λ is the X-ray wavelength and its value = 0.15056 nm, FWHM (β) is the full width at half maximum of the peak, and θ is diffraction angle (deg.).

It was observed that the average crystal size of the R-MWCNTs and F-MWCNTs are (3.27, 3.19 nm), respectively. The average crystalline size of the ZnO/F-MWCNTs is about 23.73 nm.

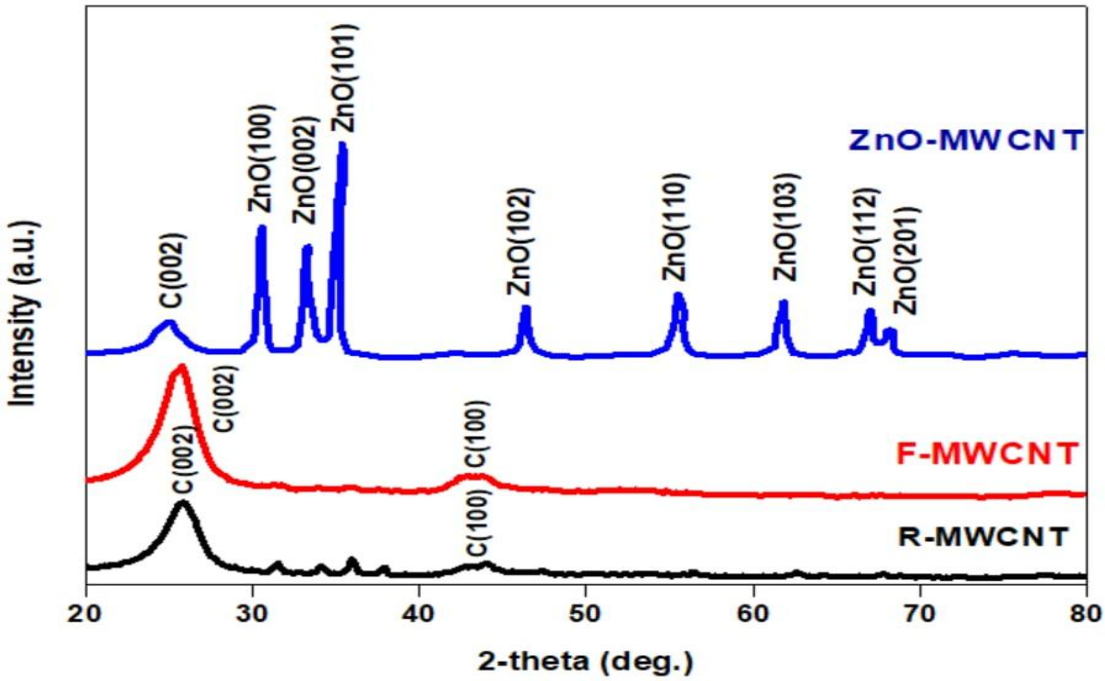

Figure 2: XRD spectra of R-MWCNTs, F-MWCNTs, and ZnO/MWCNTs hybrid.

Figure 3 a & 3 b displays the FE-SEM images of the R- MWCNTs before the acid treatment. It was noticed that the R-MWCNTs appears as cylindrical tubes shape with different directions. In addition, the particles tend to agglomerate according to Van der Waals forces between the tubes. After the acid treatment of the F-MWCNTs, it was notable that there was a significant difference in the FE-SEM image as shown in Figure 4 a & 4b. The microscopic images indicate the appearance of nanoparticles in the shape of tangled tubes that look similar a rope. Furthermore, the F-MWCNTs tubes show shorter and have less agglomeration compared to the R-MWCNTs. Additionally, F-MWCNTs structure exhibits irregularity with defects on the surface of the tubes. The mean particle size of R-MWCNTs and F-MWCNTs is (21.06 nm, 33.99 nm), respectively [20]. Figure 5 a & 5 b represents the FE-SEM analysis of the ZnO\MWCNTs hybrid at different magnifications. It was observed that zinc oxide nanoparticles appear in the form of spherical clusters that grow on the surface of tangled tubes that represent the MWCNTs as densely and not uniform. Besides, the distribution of ZnO NPs does not occur in uniform way on MWCNTs. The strong attachment between ZnO and MWCNTs is also due to the interaction between the oxygen groups (functional groups) of both samples. As shown in the image, the hybrid possesses a high surface to volume ratio, which is an important factor for catalysis or surface mediated applications [21]. The results show the success of the ZnO-MWCNTs hybrid synthesis process using the Sol-Gel method [22].

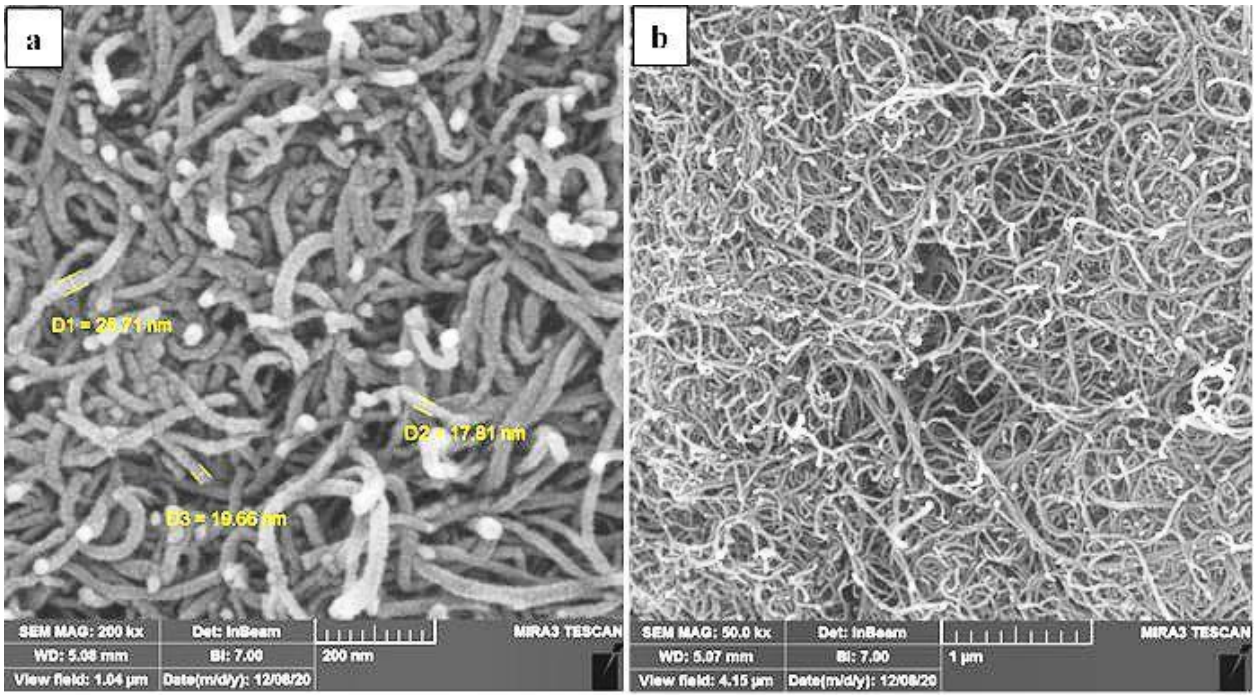

Figure 3: FESEM images of R-MWCNTs with different magnifications at a) scale bar = 200 nm and b) scale bar = 1 µm.

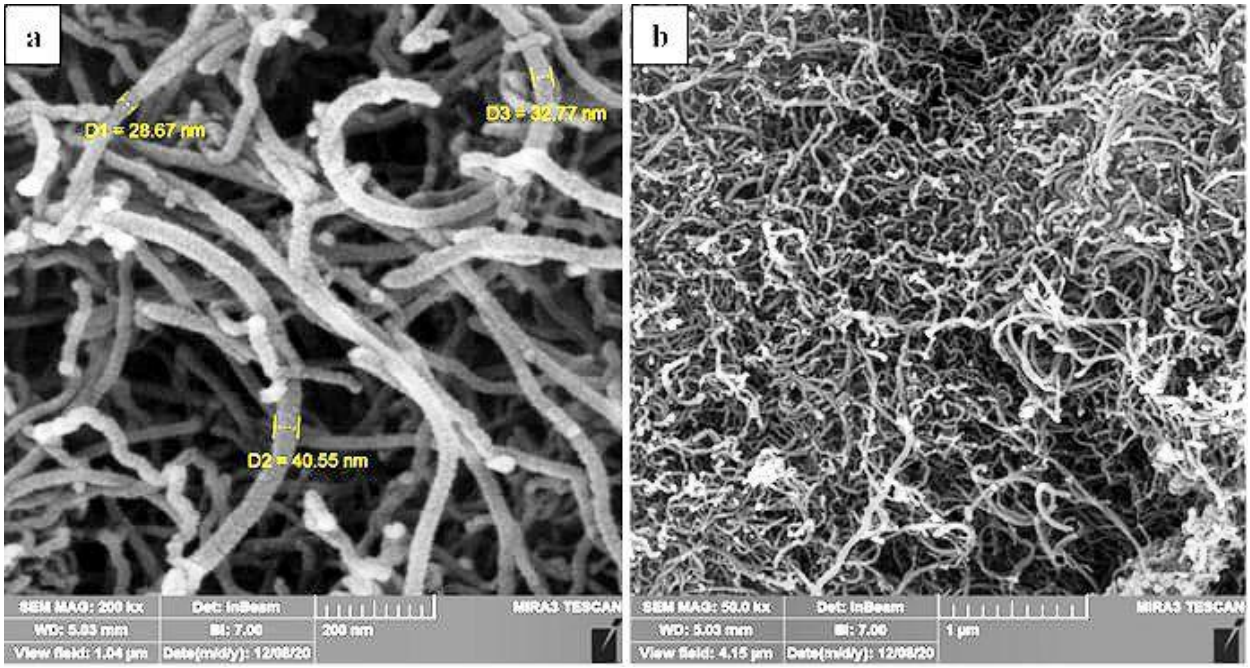

Figure 4: FESEM images of F-MWCNTs with different magnifications at a) scale bar = 200 nm and b) scale bar =1 µm.

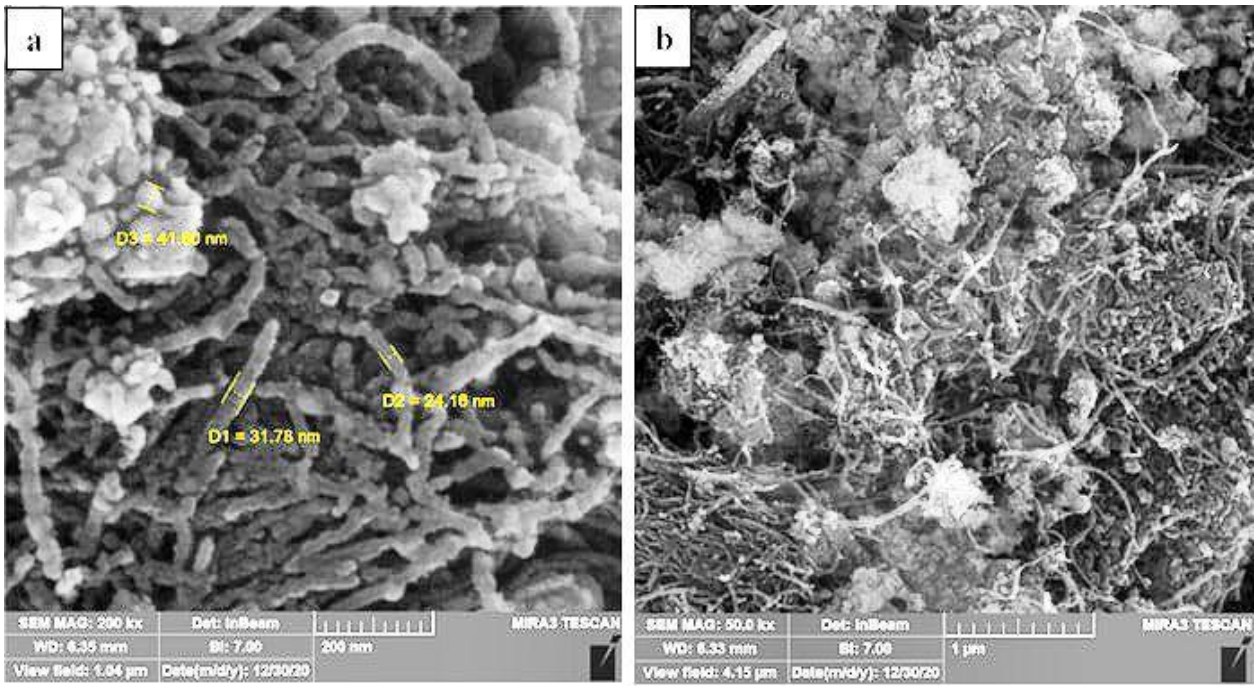

Figure 5: FESEM images of ZnO-MWCNTs hybrid with different magnifications a) at scale bar = 200 nm and b) scale bar =1 μm.

The UV-Vis spectra of R-MWCNT displays a broad absorption band at a wavelength of 291 nm attributable to the π-π* electronic transitions of the C=C bonds forming the aromatic rings in the MWCNT structure. After acid treatment of the F-MWCNT, the UV-Vis spectra display a shifting to shorter wavelength (blue shift) for the absorption peak at 264 nm. Figure 6 a shows the blue-shift region. These shifts in the absorption peak are due to changes in the density of states of electronic structure of F-MWCNTs after covalent functionalization method could lead to disruption in the aromatic system [23, 24]. Finally, the absorption spectrum of ZnO-MWCNT hybrid illustrates two absorption peaks at wavelength of 282nm, which is due to the π-π* electron transitions of the double bonds in the MWCNTs composition. Whereas, the absorption peak at 334 nm is due to the electron transitions in the Zn-O bond. This indicates the strong interaction between ZnO and the MWCNTs and thus the formation of the hybrid materials. In state of measurement, the optical energy band gap (E_g) for all samples can be calculated by Tauc's equation 2 [25]:

$$(\alpha h\upsilon)^2 = A\,(h\upsilon - E_g) \qquad \text{..... (2)}$$

Where hν is the photon energy, E_g is the optical energy band gap, and A is a constant. Bedsides, the optical band gaps (E_g) of R-MWCNT, F-MWCNT and hybrid materials have been calculated by using plotting $(\alpha h\nu)^2$ versus the incident photon energy (hν) as shown in Figure 6 b. It was found that the energy band gap values determined from the Tauc's equation eq. 2 for the R-MWCNT and F-MWCNT is up to 3.28 and 3.18 eV, respectively.

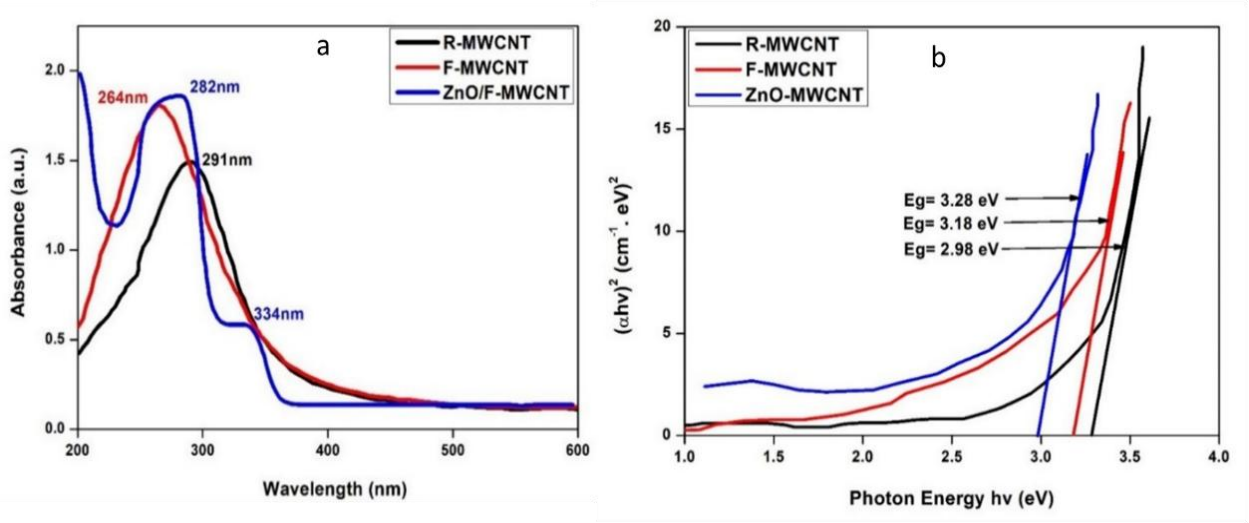

Figure 6: a) Optical absorption spectra of R-MWCNTs, F-MWCNTs, and ZnO\MWCNT hybrid. b) Plots of (αhv) 2 as a function of photon energy (E_g) for R- MWCNTs, F-MWCNTs, and ZnO/MWCNTs hybrid.

In addition, the MWCNT with ZnO NPs, exhibits a significant decrease in the energy band gap and was observed to be up to 2.98 eV. The decrease in the band gap after the association of the MWCNT with ZnO NPs is related the ability of the MWCNT to act as electron acceptors. The results undoubtedly related to the band gap shift due to the quantum confinement effect of ZnO decorated F-MWCNTs.

The antibacterial activity of R-MWCNTs, F-MWCNTs and hybrid materials initially was tested by using well diffusion method [26]. Figures 7 a, 7 b, 7 c, Figure 8 a, 8 b, 8 c and Figure 9 a, 9 b, 9 c show the photographs results of antibacterial test at different concentrations (500, 750, 1000 µg/ml) of R-MWCNTs, F-MWCNTs and hybrid samples against gram negative *E. coli* and gram positive *S. aureus* bacteria by determining the inhibition zone (IZ) in mm.

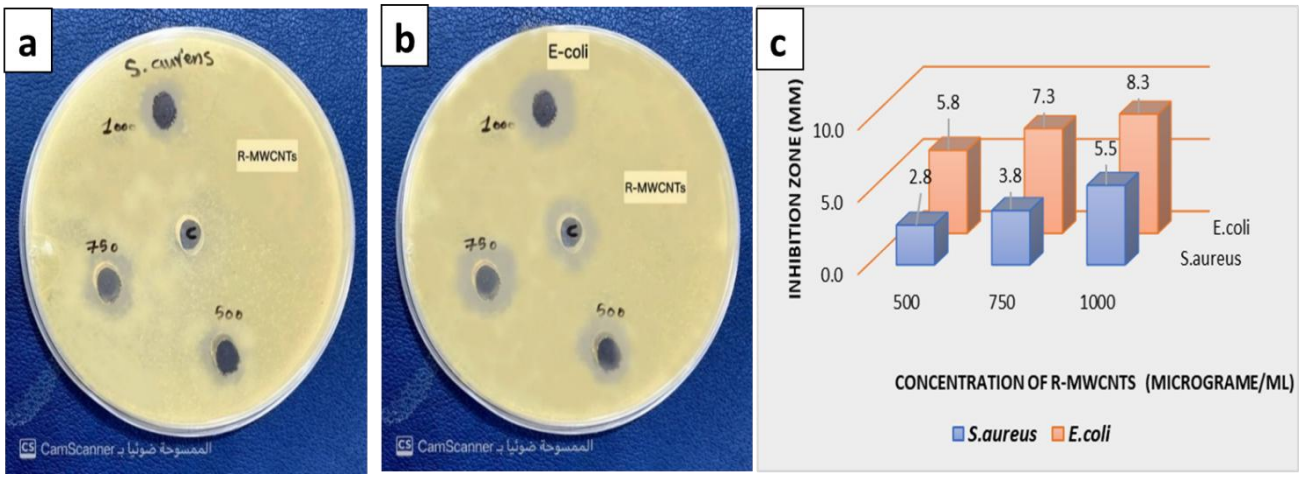

Figure 7: Inhibition Zone diameter (IZ) around well filled with different concentrations of antibacterial R-MWCNTs against a) *S. aureus*, b) *E. coli* and c) Bar diagram of antibacterial R-MWCNTs.

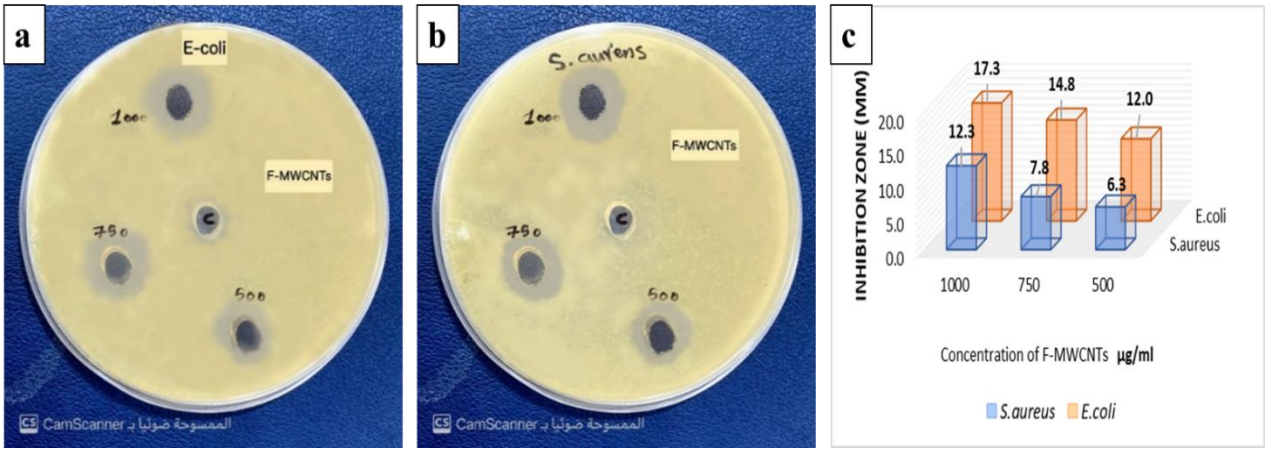

Figure 8: Inhibition Zone diameter (IZ) around well filled with different concentrations of antibacterial F-MWCNTs a) *S. aureus*, b) *E. coli* and c) the Bar diagram of antibacterial F-MWCNTs.

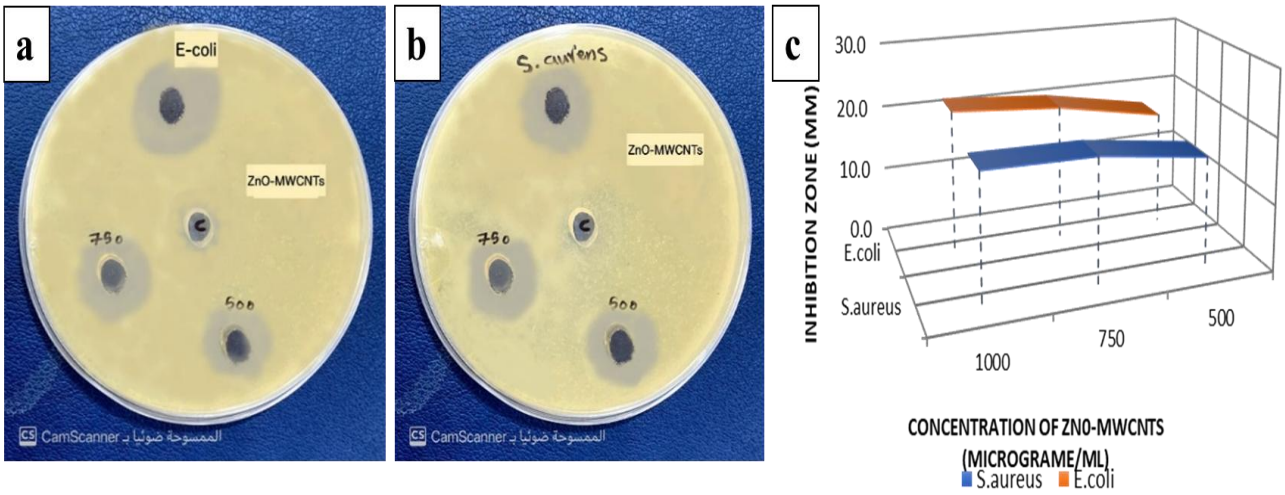

Figure 9: Inhibition Zone diameter (IZ) around well filled with different concentrations of antibacterial ZnO-MWCNTs hybrid a) *S. aureus*, b) *E. coli* and c) Bar diagram of antibacterial ZnO\MWCNTs hybrid.

The results demonstrate that F-MWCNTs and ZnO\MWCNTs hybrid recorded highest IZ (17.3 mm and 22.5 mm) for *E. coli* and IZ (12.3 mm and 19 mm) for *S. aureus*, respectively at 1000 µg/ml of each sample after incubation overnight.

4. Conclusions

In summary, ZnO\MWCNTs hybrid was prepared using the sol-gel method. Then, X-ray diffraction showed that the presence of functional oxygen groups that increase the interlayer distance between the F-MWCNTs layers. This reveals the success of the functional process using sulfuric and nitric acid without altering the structure of the F-MWCNTs. It was observed that the average crystal size of the ZnO\MWCNTs hybrid, R-MWCNTs and F-MWCNTs are (32.73 nm, 3.27 nm, 3.19 nm), respectively. The FE-SEM images showed that the F-MWCNTs tubes are shorter and have less agglomeration compared to the R-MWCNTs. Additionally, F-MWCNTs structure exhibited irregularity with defects on the surface of the tubes. The hybrid possesses a high surface to volume ratio, which is an important factor for catalysis or surface mediated applications that the average particle size of ZnO MWCNTs hybrid, R-MWCNTs and F-MWCNTs are (32.51 nm, 21.06 nm, 33.99 nm), respectively. The UV-Vis spectra showed that the band gap for the R-MWCNT and F-MWCNT was up to 3.28 and 3.18 eV, respectively. In addition, the MWCNT with ZnO NPs show a significant decrease in the energy band gap with up to 2.98 eV. Antibacterial test at different concentrations (500, 750, and 1000 µg/ml) of R-MWCNTs, F-MWCNTs and hybrid samples against *E. coli* and *S. aureus* bacteria by determining the inhibition zone (IZ) in

mm. Finally, results demonstrate that F-MWCNTs and ZnO\MWCNTs hybrid recorded highest IZ (17.3 mm and 22.5 mm) for *E. coli* and IZ (12.3 mm and 19 mm) for *S. aureus*, respectively at 1000 µg/ml of each sample after incubation overnight.

Acknowledgement

We are grateful to Medical Lab. Technique in Al-Esraa University Collage for their support of the work by making the biological tests in the Labs available and by providing the protocol of the tests.

Conflict of Interest

The authors declare that they have no conflict of interest.

References

[1] C. P. Poole Jr, and F. J. Owens, Introduction to nanotechnology: John Wiley & Sons, 2003.
[2] E. T. Thostenson, Z. Ren, and T.-W. Chou, "Advances in the science and technology of carbon nanotubes and their composites: a review," *Composites science and technology*, vol. 61, pp. 1899-1912, 2001.
[3] M. Trojanowicz, "Analytical applications of carbon nanotubes: a review," *TrAC trends in analytical chemistry*, vol. 25, pp. 480-489, 2006.
[4] L. Agüí, P. Yáñez-Sedeño, and J. M. Pingarrón, "Role of carbon nanotubes in electroanalytical chemistry: a review," *Analytica chimica acta*, vol. 622, pp. 11-47, 2008.
[5] X. Ren, C. Chen, M. Nagatsu et al., "Carbon nanotubes as adsorbents in environmental pollution management: a review," *Chemical Engineering Journal*, vol. 170, pp. 395-410, 2011.
[6] N. Yang, X. Chen, T. Ren et al., "Carbon nanotube-based biosensors," *Sensors and Actuators B: Chemical*, vol. 207, pp. 690-715, 2015.
[7] K. A. Wepasnick, B. A. Smith, J. L. Bitter et al., "Chemical and structural characterization of carbon nanotube surfaces," *Analytical and bioanalytical chemistry*, vol. 396, pp. 1003-1014, 2010.
[8] C.-S. Huang, C.-Y. Yeh, Y.-H. Chang et al., "Field emission properties of CNT–ZnO composite materials," *Diamond and related materials*, vol. 18, pp. 452-456, 2009.
[9] B. Zhang, R. Shi, Y. Zhang et al., "CNTs/TiO_2 composites and its electrochemical properties after UV light irradiation," Progress in Natural Science: *Materials International*, vol. 23, pp. 164-169, 2013.
[10] Y. Cheng, J. Huang, H. Qi et al., "Adjusting the chemical bonding of SnO_2-CNT composite for enhanced conversion reaction kinetics," *Small*, vol. 13, pp. 1700656, 2017.
[11] X. Cui, Y. Wang, G. Jiang et al., "The encapsulation of CdS in carbon nanotubes for stable and efficient photocatalysis," *Journal of Materials Chemistry A*, vol. 2, pp. 20939-20946, 2014.
[12] A. M. Eman, M. Dawya, A. Abouelsayedb et al., "Synthesis and Characterization of Multi-Walled Carbon Nanotubes Decorated ZnO Nanocomposite" *Egyptian Journal of Chemistry*, vol. 59, pp.1061-1068, 2016.
[13] Z. L. Wang, "Zinc oxide nanostructures: growth, properties and applications," *Journal of physics: condensed matter*, vol. 16, pp. R829, 2004.
[14] V. Ischenko, S. Polarz, D. Grote et al., "Zinc oxide nanoparticles with defects," *Advanced functional materials*, vol. 15, pp. 1945-1954, 2005.
[15] M. J. Osmond, and M. J. Mccall, "Zinc oxide nanoparticles in modern sunscreens: an analysis of potential exposure and hazard," *Nanotoxicology*, vol. 4, pp. 15-41, 2010.
[16] A. Becheri, M. Dürr, P. L. Nostro et al., "Synthesis and characterization of zinc oxide nanoparticles: application to textiles as UV-absorbers," *Journal of Nanoparticle Research*, vol. 10, pp. 679-689, 2008.
[17] D. Saadi, A. Abed, A. Bohan, J. Rbat, "Effect of (ZnO/MWCNTs) hybrid concentrations on microbial pathogens removal", *Engineering and Technology Journal*, vol.33, pp.1402-1411, 2015.

[18] T. Dietl, "A ten-year perspective on dilute magnetic semiconductors and oxides," *Nature materials*, vol. 9, pp. 965-974, 2010.
[19] S. Yick, A. Mai-Prochnow, I. Levchenko et al., "The effects of plasma treatment on bacterial biofilm formation on vertically-aligned carbon nanotube arrays," *RSC Advances*, vol. 5, pp. 5142-5148, 2015.
[20] A. Zaman, T. U. Rashid, M. A. Khan et al., "Preparation and characterization of multiwall carbon nanotube (MWCNT) reinforced chitosan nanocomposites: effect of gamma radiation," *BioNanoScience*, vol. 5, pp. 31-38, 2015.
[21] B. Liu, and H. C. Zeng, "Fabrication of ZnO "dandelions" via a modified Kirkendall process," *Journal of the American Chemical Society*, vol. 126, pp. 16744-16746, 2004.
[22] D. Saravanakkumar, S. U. Devi, S. S. S. Gnanasaravanan et al., "Structural Investigation on Synthesized Ag Doped ZnO-MWCNT and Its Applications," Journal of Nano science, *Nano engineering & Applications*, vol. 8, pp. 2321-5194, 2018.
[23] X. Cheng, J. Zhong, J. Meng, "Characterization of multiwalled carbon nanotubes dispersing in water and association with biological effects," *Journal of Nanomaterials*, vol. 2011, pp.1-12, 2011.
[24] H. Cui, X. Yan, M. Monasterio et al., "Effects of various surfactants on the dispersion of MWCNTs-OH in aqueous solution," *Nanomaterials*, vol. 7, pp. 262, 2017.
[25] M. A Al-Kinani, A. Haider Sharafaldin Al-Musawi., "Study the Effect of Laser Wavelength on Polymeric Metallic Nanocarrier Synthesis for Curcumin Delivery in Prostate Cancer Therapy: In Vitro Study," *Journal of Applied Sciences and Nanotechnology*, vol. 1, pp.43-5, 2021.
[26] N. Hussein M., Khadum., "Evaluation of the Biosynthesized Silver Nanoparticles'' Effects on Biofilm Formation," *Journal of Applied Sciences and Nanotechnology*, vol. 1, pp.23-31,2021.